Assessment study of a Domain-Decomposition strategy for marine applications.

M. Greco[1,2,3] **G. Colicchio**[1,2] **C. Lugni**[1,2]
m.greco@insean.it **g.colicchio@insean.it** **c.lugni@insean.it**

1 **INSEAN, Italian Ship Model Basin, Roma – Italy.**
2 **Centre for Ships and Ocean Structures (CeSOS), NTNU, Trondheim – Norway.**
3 **Department of Marine Technology, NTNU, Trondheim – Norway.**

Greco *et al.* (2011) tried to identify the proper numerical choices for the development of a three-dimensional Domain-Decomposition (DD) strategy. It aims to study the violent interaction of FPSO ships with head-sea regular waves. The present work represents a contribution in this direction. The under development DD solver combines a Boundary Element Method (BEM) for the global linear seakeeping analysis in frequency domain with a Navier-Stokes (NS) method for the flow investigation in an inner sea region containing the forward portion of the vessel. In this region, water shipping and slamming events can be caused by the liquid-structure interactions, while it is assumed that the rest of the fluid domain can be suitably described by the linear potential-flow solver. Within the NS solver, a Projection method is adopted with a finite-difference scheme on an Eulerian grid and a Predictor-Corrector scheme for the time evolution. The solver is accurate to the second order. The evolution of the free surface is captured by means of a Level-Set (LS) technique updating in time the normal distance (with-sign) from the water-air interface. Moreover the influence of the air on the water is neglected and the velocity field is smoothly extended from the liquid to the gas domain. The non-slip body-boundary condition is enforced through a hybrid Eulerian-Lagrangian approach combining the body LS function ϕ_{body} (positive in the fluid) with point markers moving with the body and initially defined on a uniform grid four times finer than the minimum mesh size in the computational grid and within a band across the body surface six times larger than the maximum mesh size of the computational grid. The body points evolve in time carrying with them their distance from the body surface and this allows a more accurate estimate of ϕ_{body} on the Eulerian grid by interpolation from the markers. The coupling between the outer and inner solvers is implemented as a weak and a strong strategy. In the former case, the information travels from the outer to the inner solver but not *vice versa*; in the latter, the information travels back and fourth. The NS solver needs initial and boundary conditions in terms of velocity, pressure and free surface elevation in the fluid and the body-boundary condition along the solid surface. The seakeeping solver feels the nonlinearities and possible viscous effects predicted in the inner domain through local and global loads acting on the ship portion inside this region. The rest of the ship hull is assumed to be subjected to the loads provided by the potential-flow outer solver. For a freely-floating vessel, the inner-domain global loads are introduced in the body-motion equations, so that the ship motion can be affected by the inner-flow features that can alter the flow pattern in the inner domain in return.

The study in Greco *et al.* (2011) examined the application of the DD strategy to a patrol ship tested at CNR-INSEAN without forward speed and highlighted numerical challenges. They are connected with the boundary conditions of the inner domain and with the prediction of the body loads by the NS solver. Within that investigation, the loads on the

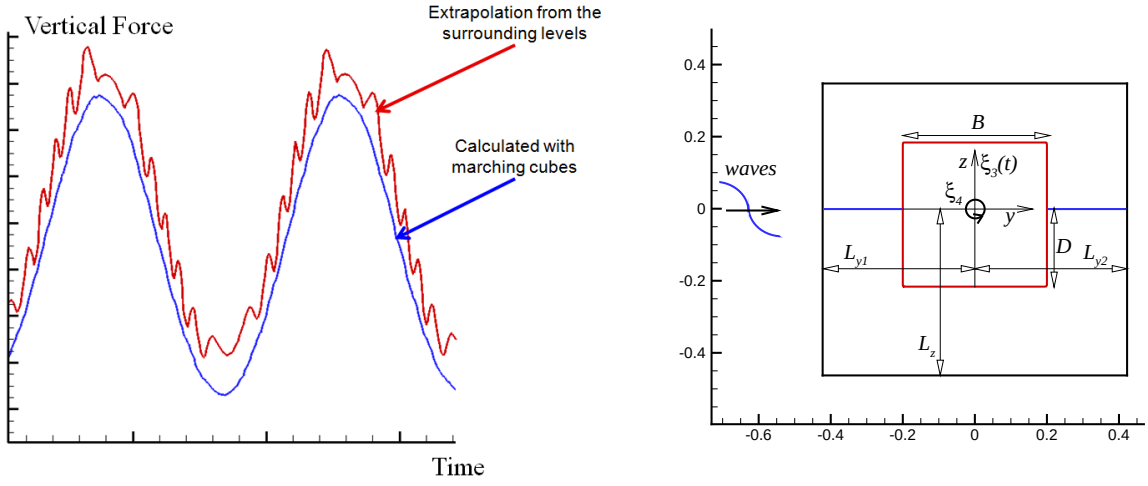

Figure 1: Weak coupling. Left: forced-heave problem for a patrol ship. Vertical force on the ship portion inside the inner domain as estimated by extrapolation and interpolation with marching-cube algorithm. Oscillation period corresponding to a wavelength $\lambda \simeq 1.25L$ and motion amplitude $\xi_{3a}/D = 0.1$. $\Delta x/L = 0.006$. Right: definition of the examined 2D problem. $B/D = 2$.

body surface were approximated as a parabolic extrapolation from the loads estimated at the three iso-surfaces $\phi_{body} = 0.5\Delta x, \Delta x$ and 1.5 Δx outside of the ship. This approach proved to be not optimal for moving bodies because of numerical oscillations induced by errors in extrapolating the pressure not exactly normally to the body surface. Therefore another strategy has been identified: the body pressure is interpolated on the vertices of the triangles that identify the body surface, then it is integrated along each triangle. The triangles are identified at any needed time instant through the marching-cube scheme searching for the intersections of each grid cell with the body surface. This avoids the temporal oscillations in the integrated loads, the back side of the medal is given by greater CPU-time requirements. Left plot of figure 1 shows a typical comparison between the results from the two methods in terms of the vertical force for a forced-heave case of the patrol ship considered in Greco *et al.* (2011). The results show that the two approaches are associated with a different buoyancy contribution (included in the vertical force) and confirm a behavior free from fictitious oscillations when using the developed interpolation method. A major change relative to the preliminary work in Greco *et al.* (2011) concerns the boundary conditions for the inner domain bounded within a parallelepiped. A careful analysis has shown that the most robust and effective strategy is an inflow condition for the free-surface elevation, the pressure p and the velocity $\boldsymbol{u}$ spread in, respectively, six, two and six cells closest to the vertical boundaries. The first two variables are sharply enforced from the BEM while the velocity passes linearly from the BEM to the NS solution. If the boundary is crossed by the body, a mixed condition is applied for the velocity: the inflow condition is modified smoothly into an outflow condition going close to the body surface to avoid inconsistency between the free-slip condition from the BEM and the no-slip condition from the NS solver. On the bottom boundary the BEM p and $\boldsymbol{u}$ are sharply enforced on the first cell.

To help the assessment of the numerical choices for the body-load predictions and for the enforcement of the inner-domain boundary conditions, the 2D geometry in the right of figure 1 has been examined in the case of diffraction of regular incident waves and radiation caused by periodic forced heave ξ_3 and roll ξ_5 motions assuming beam B=0.4 m and draft D=0.2 m. For this problem, the DD is used as a weak-coupling strategy: the 3D BEM solver is applied to a cylinder long $L = 5B$ and provides the initial and boundary conditions to the NS-LS solver describing the flow in the central cross-section plane. The inner domain has $L_{y1} = 1.5B, 2.15B$ $L_{y2} = 0, 1.5B, 2.15B$, $L_z = 4.3B$, and was studied using $\Delta y = 0.025B$. The frequency ω is set as 0.6, 0.8, 1 and 1.2 $\sqrt{2g/B}$. In the diffraction problem, the incident wave amplitude is set as $A = 0.1D$ and, in the radiation problems, the oscillation amplitudes $\xi_{3a} = 0.05D = 0.01$m and $\xi_{4a} = 0.05$ rad are considered. The results are given in figure 2 using $L_{y1} = L_{y2} = 2.15B$. These choices lead to linear conditions which can be challenging for CFD methods because the results are very sensitive to the numerical accuracy. The solid and dashed lines in the plots represent the potential-flow solution; in particular, the 3D and 2D data are obtained integrating, respectively, along the whole BEM cylinder with $L = 5B$ and along a central strip wide $1.25B$. But for b_{44}, the DD results are globally consistent with the 2D BEM results and confirm a dominant linear potential-flow behavior for the studied conditions. Viscous effects connected with friction along the body and with the vortex shedding caused by the small radius of curvature at the bottom edges of the cross-section can partially explain the larger values of the DD results for b_{44}. The instantaneous vorticity field in the case of forced roll is examined in figure 3 as a function of the oscillation frequency. As ω increases more intense vortical structures are shed from the body and the previous oscillation vorticity is still visible in the fluid field. An exception is $\omega = 0.8\sqrt{2g/B}$ which is associated with the lowest vorticity. The 2D numerical results in figure 2 are close to the experimental data by Vugts (1968), also given in the figure, with the largest discrepancies in the region of low ω. There, the model tests are quite consistent with the 3D BEM results. Though the physical cylinder was much longer ($L = 10.475B$) than in the BEM simulations, this suggests possible 3D effects in the experiments. The model tests are associated with an added-mass in roll much lower than the numerical results. This is possibly due to experimental errors in calculating the roll added mass, as pointed out by Vugts (1968). In the experiments it was difficult the properly estimate the moment of inertia and this led to a_{44} smaller than in reality. For the heave motion, a larger amplitude $\xi_{3a} = 0.15D = 0.03$m is also examined in figure 2. The added-mass and damping coefficients from the experiments and the DD appear consistent and show that a_{33} is dominated by linear effects while b_{33} shows some nonlinearities as ω increases.

To assess the numerical choices made in the case of a body crossing the inner-domain boundary, L_{y2} has been set to zero so that only half of the body is inside the NS-LS domain in its mean configuration. The results are given in the top plots of figure 4 for the case of heave with amplitude $\xi_{3a} = 0.15D$ and $\omega = 0.6\sqrt{2g/B}$. The vertical force on half of the domain is consistent with half of the force acting on the whole body (left plot). On the other hand, as expected, near the right overlapping region between the BEM and the NS-LS domains the pressure field deviates from the viscous-flow solution. The results indicate that, within a strong-coupling analysis of a seakeeping problem, to be on the safe side the loads from the NS-LS solver should be obtained integrating on a portion of the body sufficiently inside the inner domain, say with a distance greater than the overlapping thickness (6 cells) *plus* four extra cells. A part from this area near the boundary, the pressure fields in the two cases are consistent. Similar agreement is also observed in the case of forced roll motion with $\xi_{5a} = 0.05$ rad and $\omega = 0.6\sqrt{2g/B}$, as shown in the bottom-left plot of figure 4. The pressures near the right boundary of the narrower domain are more consistent for the two simulations than in the case of the forced heave. This can be intuitively understood because the roll gives a motion normal to the boundary while the heave leads to a motion parallel

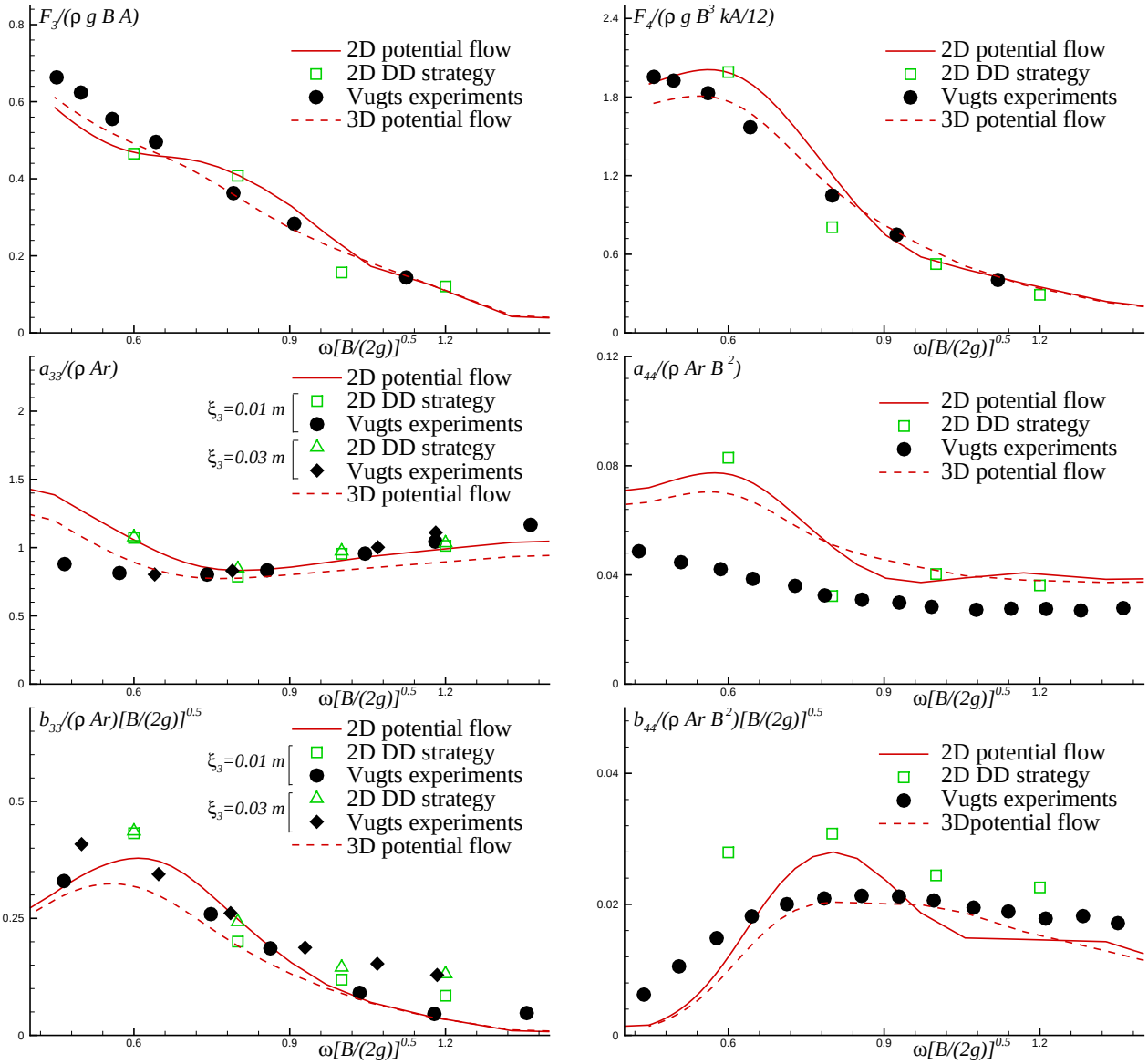

Figure 2: Top: heave (left) and roll (right) wave exciting loads. Center: added-mass in heave (left) and roll (right). Bottom: damping in heave (left) and roll (right). $Ar = 0.9992BD$ is the cross-section area. ($L_{y1} = L_{y2} = 2.15B$)

to the boundary and so with larger sensitivity to the NS-LS and BEM description of the flow-boundary solution (velocity and pressure must be furnished in an area seen as inside the body by the linear potential solution). The bottom-right plot of the figure examines the influence of the domain horizontal dimensions for the same forced-roll conditions. In this case the body is inside the NS-LS domain in both simulations. The narrower-domain solution shows some unphysical behavior of the pressure near the left boundary but it is quite consistent with the wider-domain solution elsewhere. Instead, the velocity field is more sensitive to the closeness of the boundary and appears somewhat different than the wider-domain solution even besides the body surface. One must then identify the minimum L_{y1} and L_{y2} to ensure a physical solution near the body. It should be noted that the difference in the velocity is not much felt by the roll moment acting on the body (not shown here). An even more critical parameter is L_z. On the bottom, the inconsistency between the irrotational potential flow and the rotational NS-LS can act like a porous boundary, influencing the detachment and evolution of the shed vorticity. This must be avoided either by dynamically enlarging the inner-domain extension or by introducing a numerical diffusivity of the vorticity near the domain boundary and sufficiently far from the body so that the physical phenomena relevant for the liquid-structure interactions are correctly described. A parameter analysis is ongoing, aiming to obtain the proper dimensioning of the inner domain as a function of the type and amplitude of motion and will be presented at the workshop. The details of the developed DD solver are described in Greco *et al*. (2012) and will be also discussed at the workshop.

This research activity is supported by the Centre for Ships and Ocean Structures (CeSOS), NTNU, Trondheim, within the

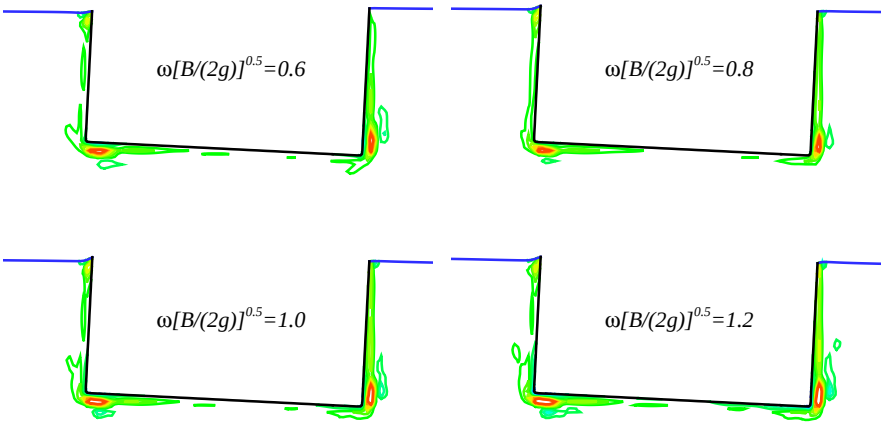

Figure 3: Forced roll motion with $\xi_{5a} = 0.05$ rad: vorticity contours for $\omega =$ 0.6, 0.8, 1.0 and 1.2 $\sqrt{2g/B}$. Snapshot corresponding to maximum ξ_5. ($L_{y1} = L_{y2} = 2.15B$)

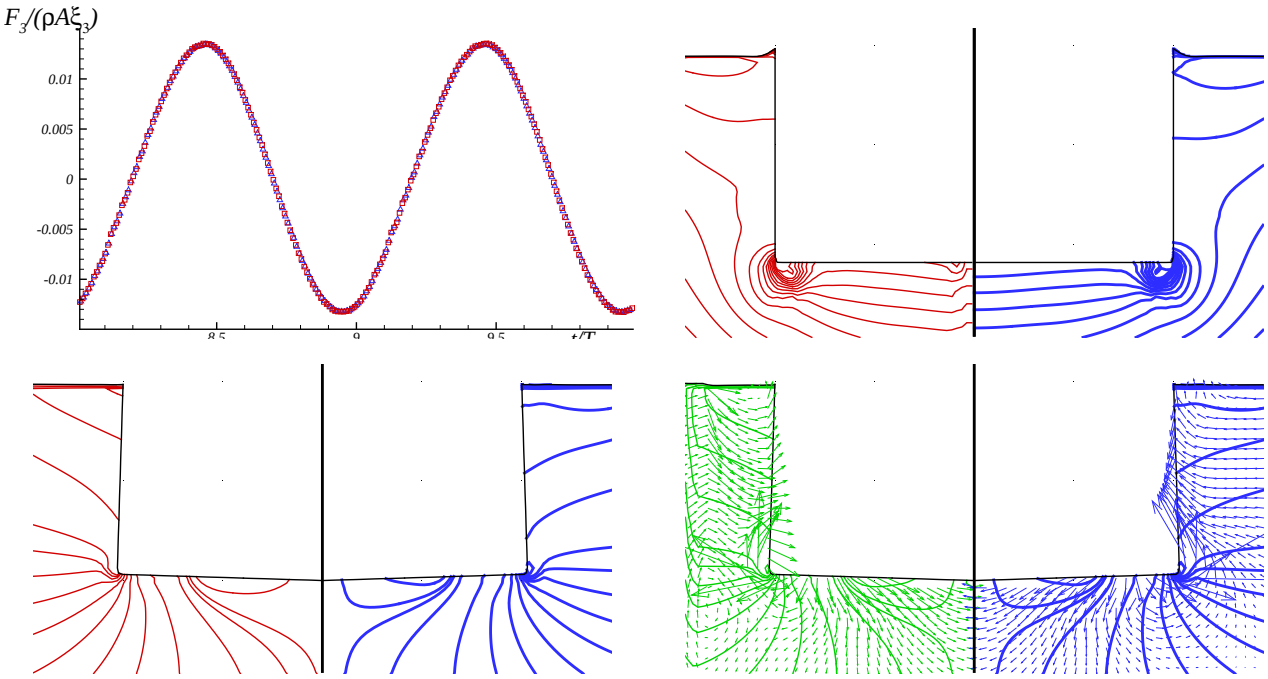

Figure 4: Top: forced heave motion with $\xi_{3a} = 0.15D$ and $\omega = 0.6\sqrt{2g/B}$. Vertical force (left) and pressure field (right) using $L_{y2} = 0$ (half left) and $L_{y2} = 2.15B$ (half right). Bottom: forced roll motion with $\xi_{5a} = 0.05$ rad and $\omega = 0.6\sqrt{2g/B}$. Pressure field (left) using $L_{y2} = 0$ (half left) and $L_{y2} = 2.15B$ (half right) and pressure and velocity fields (right) using $L_{y1} = L_{y2} = 1.5B$ (half left) and $L_{y1} = L_{y2} = 2.15B$ (half right).

”Violent Water-Vessel Interactions and Related Structural Loads” project.

References

GRECO, M., G. COLICCHIO, AND C. LUGNI (2011). Development of a 3D Domain-Decomposition strategy for violent head-sea wave-vessel interactions: Challenges. In 26^{th} *Int. Workshop of Water Waves and Floating Bodies*, Athens, Greece.

GRECO, M., G. COLICCHIO, C. LUGNI, AND O. FALTINSEN (2012). 3D Domain Decomposition for Violent Wave-Ship Interactions. *Manuscript in preparation*.

VUGTS, J. (1968). The hydrodynamic coefficients for swaying, heaving and rolling cylinders in a free surface. *Int. Ship-building Progr. 15*.